Sudan University of Science and Technology
College of Graduate Studies

Structural and Optical Properties of ZnO Nano-Powder Synthesized by Combustion and Sol-gel Method

الخصائص التركيبية والبصرية لبدرة اكسيد الزنك النانوية المحضرة بطريقة الاحتراق والصل جل

A dissertation Submitted in Partial Fulfillment for the Requirement of a Master Degree (M. Sc) in Physics

by:

Mohamed Elmahi Mohamed Ahmed

Superviser:

Dr. Abd Ellateef Abbass

September 2018

الآية

قال تعالى:

اعوذ بالله من الشيطان الرجيم ، بسم الله الرحمن الرحيم

"وَمَا تَكُونُ فِي شَأْنٍ وَمَا تَتْلُو مِنْهُ مِنْ قُرْآنٍ وَلَا تَعْمَلُونَ مِنْ عَمَلٍ إِلَّا كُنَّا عَلَيْكُمْ شُهُودًا إِذْ تُفِيضُونَ فِيهِ ۚ وَمَا يَعْزُبُ عَنْ رَبِّكَ مِنْ مِثْقَالِ ذَرَّةٍ فِي الْأَرْضِ وَلَا فِي السَّمَاءِ وَلَا أَصْغَرَ مِنْ ذَٰلِكَ وَلَا أَكْبَرَ إِلَّا فِي كِتَابٍ مُبِينٍ" ﴿ ٦١ ﴾ سورة يونس ﴿61﴾

صدق الله العظيم

Dedication

I dedicate this work for:

Mom and Dad (Cherishing)

Brothers and sisters (Flavor of life)

All teachers, lovers and friends with deferent ages

Also I dedicate my research for the souls of the dears dead I missed them.

Finally the dedication for my future wife and kids (Optimism)

Acknowledgements

First and foremost, I would like to thank God, for giving me courage and strength during this research.

I would like to express my sincere appreciation to Dr. Abd Ellateef Abbass for his guidance, professional support, suggestions and encouragements.

Great thanks to Sudan University for science and technology (SUST) specially the department of Physics and Institute of Laser for their assistance and support.

The author would like to thank Prof. Kroon and Prof. Swart at the Department of physics, University of the Free State for assisting with all measurements.

Last but not the least my truthful indebtedness to my parents for their fundamental moral support.

Mohamed Elmahi

Abstract

Nowadays, ZnO is considered as the most important chemical compounds due their distinctive properties owing to its wide band gab and large exciton binding energy. It is well known that the structural and the optical properties of ZnO differ by different methods of preparation. Therefore, in this work, ZnO power was prepared by two methods, namely sol-gel and combustion method with the aim of comparison. The obtained samples from both methods were investigated by many techniques for considerable comparison.

The obtained results from ZnO synthesized by the sol- gel method showed that the crystallite size of ZnO was increases by increasing of the annealing temperature. Also little change in the lattice parameter was observed when the annealing temperature increased. It is observed also that similar structure of ZnO prepared by sol-gel and combustion can be obtained at particular conditions. TEM studies showed that the ZnO nanocrystals are irregularly spherical with average diameter of 32 nm, which is similar to the calculated crystallite size from the XRD data. The calculated energy band gab of ZnO prepared by combustion method is found to be 3.2 eV while for samples prepared by sol-gel method is found to be increased with increasing the annealing temperature.

There was a clear difference between the two PL spectra obtained from ZnO synthesized by sol-gel and combustion method which is assigned to be due to complicated defect chemistry relevant to the experimental process.

المستخلص

في الاونة الاخيرة اعتبر اكسيد الزنك من اهم المركبات الكيميائة نتيجة للخواص المميزة التي يتمتع بها بسبب اتساع فجوة الطاقة وكبر طاقة ربط الاكسيتون. وكما هو معلوم فإن خصائص المركب تختلف من طريقة تحضير لأخرى. لذلك في هذا البحث تمت دراسة الخصائص التركيبية والبصرية لأكسيد الزنك المحضر بطريقة الاحتراق وطريقة الصل جل بهدف المقارنة. كل العينات التي تم تحضيرها تم فحصها بعدد مقدر من التقنيات بهدف مقارنة اشمل.

أظهرت النتائج التي تم الحصول عليها من عينات اكسيد الزنك التي تم تحضيرها بواسطة طريقة الصل-جل أن حجم الجسيمات النانوية يزداد بزيادة درجة حرارة التلدين .أيضا كان هناك تغيير طفيف في معامل الشبيكة عند زيادة درجة حرارة التلدين .ويلاحظ أيضاً أنه يمكن الحصول على بنية مشابهة من اكسيد الزنك بأستخدام طريقة الصل- جل والاحتراق في ظروف معينة . أظهرت النتائج المتحصل عليها من المجهر الالكتروني النافذ أن حجم الجسيمات النانوية شبة كروية بمتوسط قطريساوي 32 نانومتر ، وهو يتفق مع حجم الجسيمات النانوية المحسوبة من بيانات حيود الاشعة السينية. تم حساب فجوة نطاق الطاقة لعينة اكسيد الزنك التي تم تحضيرها بواسطة طريقة الحتراق ووجدت انها تساوي 3.2 الكترون فولت بينما وجد ايضا ان فجوة نطاق الطاقة لعينة اكسيد الزنك التي تم تحضيرها بواسطة طريقة الصل-جل تزداد مع زيادة درجة حرارة التلدين. وجد ايضا ان هناك اختلاف واضح بين أطياف الفلورة التي تم الحصول عليها من عينات اكسيد الزنك التي تم تحضيرها بواسطة الصل-جل وطريقة الاحتراق حيث تم نسبها للخلل الذي يحدث في العمليات الكيميائية المعقدة المرافقة لعملية التحضير.

Keywords and Acronyms

Keywords

ZnO, Combustion, Sol-gel, Band gap energy, Photoluminescence (PL).

Acronyms

ZnO: Zinc Oxide.

Eg: Energy gab

XRD: X-ray diffraction**.**

TEM: Transmission electron microscopy**.**

UV-Vis: Ultraviolet visible spectroscopy.

PL: Photoluminescence spectroscopy.

List of Contents

List of Figures

List of Tables

Chapter One

Introduction

1.1 Overview

ZnO has attracted much attention in the last 50 years due to their promising physical properties owing to its wide band gap 3.37 eV, large bond strength, and large exciton binding energy (60 meV) at room temperature (Krongarrom, 2012) .

Naturally, ZnO is an *n*-type semiconductor material with direct band gab that displays a hexagonal crystalline *wurtzite*-type structure, with space group $P6_3mc$ and lattice parameters of a = b = 0.3250 nm and c = 0.5207 nm (Gusatti et al., 2009). The most importance characteristics of ZnO that make it desired for a wide range of applications are its high conductance, chemical and thermal stability, low cost, environmentally friendly and can be easily synthesised in different forms e.g. nanoparticles (NPs), nanorods, nano-disks, nano-cubes, etc. (Chu et al., 2000). Due to exceptional luminescent properties in the UV and visible region, ZnO has found many applications particularly in solid state blue to ultraviolet (UV) optoelectronics including laser developments (Suwanboon, 2008). Moreover, due to its non-centrosymmetric crystallographic phase, ZnO shows the piezoelectric property which is very useful in the fabrication of devicessuch as electromagnetic coupled sensors and actuator (Rodnyi et al., 2011). In addition, ZnO nanostructures (e.g. nanoparticles (NPs), nanorods, etc) has attracted considerable attention due to its intriguing properties such

as dielectric, piezoelectric, pyroelectric, semiconducting, acousto-optic, optical, electro-optical, nonlinear optical, photo-electro-chemical and electrical properties which make it desirable for possible applications in solar cell, acoustic, electrical and optical devices, chemical sensors, catalysts, pigments, cosmetics, varistors and gas sensors (Savi et al., 2012).

Many methods has been used to synthesized ZnO nanostructures, such as molecular beam epitaxy, thermal decomposition, hydrothermal, synthesis by vapor phase, precipitation, combustion, spray pyrolysis and sol-gel method (siva et al., 2013). Among the various methods, the chemical routes methods are known as suitable methods for the preparation of ZnO nanostructures due its some advantages such as low cost, high uniformity of the final product (shah et al., 2013). Furthermore, the combustion and sol-gel methods have special advantages over other techniques such as its simplicity, versatility, relatively low temperatures and low equipment cost. As the result, Combustion and Sol-gel methods are considered as good candidates for industrial production of materials oxide.

In particular, the combustion and sol-gel methods are known to produce high quality ZnO powder with high crystallinity and purity. In addition, the particle properties such as morphology and size can easily be altered via these methods by controlling the reaction temperature, concentration and reaction time (Prabhu et al., 2013). Actually, lots of reports were published regarding the structural and optical properties of ZnO synthesized by sol gel or by combustion method in separate works. However, the comparison between the structural and optical properties of ZnO synthesized by these methods has not been the focus of any studies. In

this work, undoped ZnO powder were prepared by two different methods namely sol-gel and combustion method with aim to compare the physical properties of the obtained samples. All samples were characterized using X-ray diffraction (XRD), UV-Vis spectrophotometer, Transmission electron microscope (TEM) and laser as excitation source.

1.2 Literature review

Due to its extensive applications in physics, chemistry and biology, ZnO compound have attracted great interest in the recent scientific research. Actually, ZnO can be synthesized by many different methods such as molecular beam epitaxy, thermal decomposition, hydrothermal, synthesis by vapor phase, precipitation, spray pyrolysis, sol-gel and combustion method (Nghia et al., 2012)**.** Among the above mentioned methods, the Sol-gel and combustion methods are the common used methods due to their simplicity, low cost, versatility, relatively low temperatures and fast preparation. Moreover, they known to produce ZnO powder with the same purity desired. There are many researches in literature reported synthesis of ZnO by these two methods. For example (Prabhu et al., 2013) reported synthesis of ZnO nanopowders by combustion method, and the obtained results showed high purity and crystallinity of ZnO with the wurtzite structure having crystallite size of 21.25 nm. The authors also calculated the band gap which was found to be 3.5 eV. In other study, D. Syamala Bai was prepared ZnO by combustion method using different fuels (glycine, citric acid, urea, and raphanus sativus [radish] extract) (Bai., et. Al). The produced ZnO showed high purity and crystallinity with the wurtzite structure.

Lots of researches also reported synthesis of ZnO by sol-gel method. For example prepared ZnO nanopowder with crystallite size between 20 and 40 nm. In 2008, also Seema Rani et al, reported synthesized of ZnO nano-powder with crystallite size of 14 nm and band gap of 3.57 eV by Sol-gel method.

1.3 Problem statement

Up to now lots of methods have been used to synthesis ZnO nanostructure. The obtained samples from these methods showed different physical properties and therefore different applications. The challenging question is how to select the preparation method for particular application. This work is expected to give more details about the samples prepared by two different preparation methods namely combustion and sol-gel in order to compare them for possible applications.

1.4 Research Objectives

1.4.1 General Objective

To investigate the effect of the preparation method on the structure and optical properties of un-doped ZnO

1.4.2 Specific Objectives

- To determine the structure properties of un-doped ZnO powders prepared by both sol-gel and combustion method using X-ray diffraction (XRD) and Transmission electron microscopy (TEM).
- To determine the optical properties of un-doped ZnO powders prepared by both sol-gel and combustion method using UV-Vis spectrometer and photoluminescence (PL) techniques.

- To compare the structural and optical properties of ZnO prepared by combustion method with ZnO prepared by sol-gel at different annealing temperatures.

1.5 Dissertation layout

This research is consist five chapters, Chapter one is about introduction and literature reviews, Theoretical background and all the properties about ZnO and applications in chapter two. Chapter three includes the experimental and characterization techniques, chapter four is about the result and discussion and finally the conclusion and recommendations of research.

Chapter Two

Theoretical Background

2.1 Overview

Zinc oxide is an in organic compound with formula ZnO. It is found naturally in the mineral called zincite. ZnO is known as binary semiconductor with direct band gap belonging to the group II-VI with a wide energy band gap (3.37 eV) and a large exciton binding energy of 60 meV at room temperature (Nghia et al; 2012). Recently, ZnO powder has attracted much attention due to its promising properties such as dielectric, piezoelectric, pyroelectric, semiconducting, acousto-optic, optical, electro-optical, nonlinear optical, photo-electro-chemical and electrical properties (Welderfael et al., 2013). Due to these exceptional properties, ZnO has been used in a wide range of applications. Details about their applications and physical properties will be given in the following sections.

2.2 Structural properties

ZnO crystallizes into three different forms, namely zinc blende (B3), wurtzite (B4) and rocksalt (B1) as schematically shown in figure 2.1. The symbols B1, B3, and B4 indicate the Strukturbericht designations for the three phases (Singh et al., 2014**).** The most common form is the wurtzite structure because is thermodynamically stable phase under ambient conditions. Zinc blende can be stabilized only by growth on cubic substrates while rocksalt structure is only stable under high pressures (Kabongo et al., 2013). In the cubic zinc blende and hexagonal wurtzite structure, each anion

is surrounded by four cations at the corners of a tetrahedron and vice versa, while the cubic rocksalt phase is crystallized in the well known NaCl structure (figure 2.1(a)).

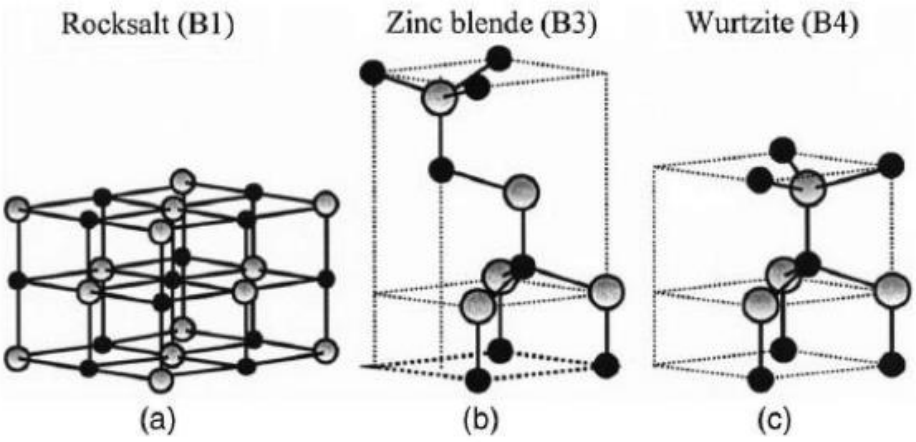

Fig. 2.1 Schematic representation of ZnO crystal structures: (a) cubic rocksalt (B1), (b) cubic zinc blende (B3), and (c) wurtzite (B4). Red and gray spheres denote Zn and O atoms, respectively (Chai et al; 2010).

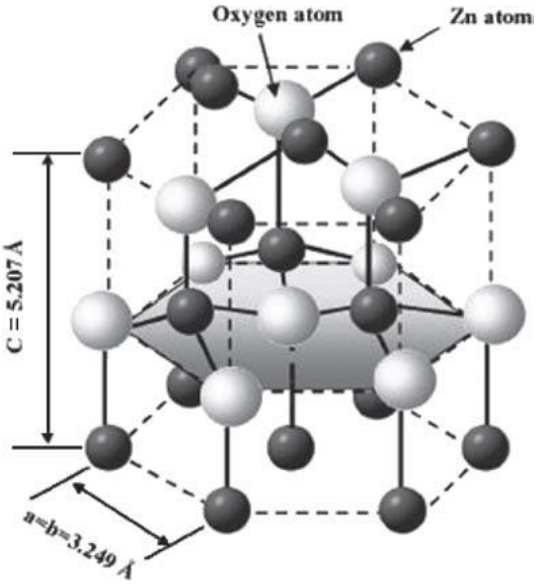

Fig. 2.2 Unit cell of the wurtzite structure of ZnO. O atoms are shown as larger white spheres while the Zn atoms are smaller brown spheres (Vaseem et al., 2010).

Figure 2.2 shows the hexagonal unit cell of the wurtzite structure which has two lattice parameters *a* and *c*. In an ideal wurtzite structure the ratio of these parameters is $c/a = \sqrt{8/3} = 1.633$ and experimentally is varies from 1.593 to 1.601 (Morkoc et al., 2008)**.** The hexagonal wurtzite structure of ZnO belongs to the space group C_{6v}^4 in the Schoenflies notation and $P6_3mc$ in the Hermann-Mauguin notation (Morkoc et al., 2008). Table 1.1 summerizes some properties of ZnO.

Table 1.1 Physical properties of ZnO (Vaseem et al., 2010).

Properties	**ZnO**
Lattice parameters at 300 K	
—a_0 (nm)	0.32495
—c_0 (nm)	0.52069
—c_0/a_0	1.602(1.633*)
Density (g/cm3_	5.606
Stable phase at 300 K	Wurtzite
Melting point (^{o}C)	1975
Thermal conductivity ($Wcm^{-1}{}^oC^{-1}$)	0.6, 1-1.2
Linear expansion coefficient (Özgür)	a_0: 6.5 cm3 × 10^{-6} c_0: 3.0 cm3 × 10^{-6}
Static dielectric constant	8.656
Refractive index	2.008
Band gap (RT)	3.370 eV
Band gap (4 K)	3.437 eV
Exciton binding energy (meV)	60
Electron effective mass	0.24
Electron Hall mobility at 300 K (cm^2/Vs)	200
Hole effective mass	0.59
Hole Hall mobility at 300 K (cm^2/Vs)	5–50

2.2.1 Scherer's Equation

The Scherer's equation is a formula that relates the size of sub-micrometre particles, or crystallites, in a solid to the broadening of a peak in a diffraction pattern (Vijayakumar, 2013). It is named after Paul Scherrer. It is used in the determination of size of particles of crystals in the form of powder.

$$D = \frac{k\lambda}{\beta cos\theta} \qquad (2.1)$$

where τ is the mean size of the crystallites, K is the shape factor, λ is the X-ray wavelength, β is the full-width-at-half-maximum (FWHM) in radians and θ is the Bragg angle.

2.2.2 Lattice Parameters

Lattice parameters can be obtained from Bragg law (Morkoc et al., 2008).

$$d_{(hkl)} = \frac{\lambda}{2 \ * \ sin\,\theta} \qquad (2.2)$$

For a hexagonal system, the relation between the lattice spacing d, the miller indices h, k, l and the cell axis (a and c) are given by the following equation (Dana et al., 1959).

$$\frac{1}{d^2} = \frac{4}{3} * \left[{(h^2 + hk + k^2)}/{a^2} \right] + \frac{l^2}{c^2} \qquad (2.3)$$

where λ is the x-ray wavelength and θ is the incident angle of x-ray.

2-3 Optical Properties of ZnO

ZnO has become one of the most promising materials for the fabrication of optoelectronic devices operating in the blue and ultraviolet (UV) (Ningthoujam et al., 2014). The optical properties of ZnO is actually

depends on the choice of the corresponding impurity and the parameters of the synthesis and subsequent treatment of the sample. As a rule, various forms of ZnO exhibit two luminescence bands, one is located in the ultraviolet region due recombination of excitons while the other is located in the visible region due to recombination of carriers trapped at deep level defects. (Suwanboon, 2008).

The UV-peak is considered to be the characteristic emission of ZnO, and is attributed to the band edge emission or the exciton transition. The broad emission appeared in the visible region is associated with the different types of intrinsic defects (Avijit Ghosh et al., 2010).

2.3.1 Determination of Energy gabs from Reflectance Spectra

The Kubelka-Munk equation at any wavelength becomes:

$$F(R_\infty) = (1 - R_\infty)^2/2R_\infty = K/S \qquad (2.4)$$

$F(R_\infty)$ is the so-called remission or Kubelka-Munk function, Where $R_\infty = R_{sample} / R_{reference}$, K is absorption coefficient and S is scattering coefficient. The optical band gap energy can be calculated from the UV absorption edge using the well-known Tauc law relation (A. Escobedo Morales, 2007)

$$\alpha h\nu = C_1(h\nu - Eg)^m \qquad (2.5)$$

Where α is the absorption coefficient, $h\nu$ is the incident photon energy, C_1 is constant, Eg is the optical band gap energy, and the exponent m is a parameter which depends on the type of electronic transition responsible for absorption. For direct band gap m equal 1/2 and 1/3 for allowed transition and forbidden transition respectively, while for indirect band gap m equal 2 and 3 for allowed transition and forbidden transition respectively.

When the material scatters in a perfectly diffuse manner, the absorption coefficient K becomes equal to 2α (K=2α). Considering the scattering coefficient S as constant with respect to wavelength, and using equations (2.4) and (2.5), the following expression can be written:

$$[F(R\infty)*h\nu]^{0.5} = C_2 (h\nu - Eg) \qquad (2.6)$$

By plotting $[F(R\infty)*h\nu]^{0.5}$ against hν and fit the linear region with a line and extend it to the energy axis, then one can easily obtained Eg by extrapolating the linear fitted regions to
$[F(R\infty)h\nu]^{0.5} = 0$ (A. F. Lima, 2009).

2-4 Mechanical Properties of ZnO

ZnO is a relatively soft material with approximate hardness of 4.5 on the Mohs scale (Hernandezbattez et al., 2008**).** Its elastic constants are smaller than those of relevant III-V semiconductors. Ultrasonic experiments on single-crystal specimens of the wurtzite (B4) phase of ZnO have shown that, under pressure, the ZnO becomes softer against shear-type acoustic distortions (Morkoc, 2008).

2-5 Electrical Properties

One of the most promising electrical properties of ZnO are its wide bandgap (approximately 3.37 eV at room temperature) and high exciton binding energy (approximately 60 meV) (Anh et al., 2014). The advantages associated with a large band gap include higher breakdown voltages, ability to sustain large electric fields, lower electronic noise, and high-power operation (Teng et al., 2006).

2-6 Native type of Defects in ZnO

The native defects in ZnO include Oxygen vacancies (V_O), Zinc vacancies (V_{Zn}), Zinc interstitials (Zn_i), Oxygen interstitials (O_i) and antisites (ZnO and OZn). Several studies claim that such native defects create shallow donor states and suggested that Zn_i are the main cause for n-type conductivity rather than V_O (Wu et al). However, more recent theoretical and experimental studies argue that Zn_i are unstable and diffuse at room temperature, while V_O are deep compensating defects and therefore are responsible for the n-type conductivity. Instead these studies suggest that hydrogen and group III elements impurities are more likely to be responsible for the n-type conductivity in ZnO. Actually, these types of defects are not yet clearly understood and therefore their emission has not been clearly delineated.

2-7 Applications of ZnO

ZnO has a wide range of applications due to its promising physical properties mentioned above. In material science applications, zinc oxide can be used in nonlinear optical devices, sensors, energy generators, and light - emitting diodes, lasers, in transparent electrodes, liquid, crystals displays, solar cells and others optoelectronics (Vaseem et al., 2010). Moreover, ZnO is also added to materials and products including plastics, ceramics, glass, cement, rubber manufacture, lubricants, paints, ointments, adhesive, sealants, concrete manufacturing, batteries, ferrites, fire retardants, coatings to enhance their properties (Park et al., 2004). In chemistry, ZnO is commonly used as photo catalysis. ZnO has a lot of uses in Medicine. It's

widely used to treat a variety of skin conditions, including dermatitis, itching due to eczema, diaper rash and acne (McNeil et al., 2005). ZnO also used in biology as antibacterial and UV-protection properties. ZnO has other uses in foods additive, UV absorber, Cigarette filters, Corrosion prevention in nuclear reactors, Methane reforming (Chai, 2010).

Chapter Three

Experimental and Characterization techniques

3.1 Experimental

Many methods of preparing ZnO have been used such as combustion, sol-gel, solid state reaction, hydrothermal, microwave process, spray pyrolysis and precipitation method. ZnO with low cost and high efficiency require simple synthesis methods at low temperature to produce small particle size. Combustion and sol-gel methods are a good choice because they both meet the mentioned requirements.

3.1.1 Sol-gel method

The sol-gel process is a wet chemical technique widely used in the fields of ceramics engineering and materials science. In this method, highly reactive compounds are used as initial precursors. These precursors are generally metal alkoxides M (OR)x, where M is a metal (M = Zr, Ti, Fe, Ni) or a transition metal (M = Si, Sn) atom and R is an alkyl group (R = Me, Et, Pr...).

In this work, pure ZnO was prepared by sol-gel method (precipitation). Zinc nitrate hexahydrate (Zn $(NO_3)_2.6H_2O$, 98%) and (NaOH, 98%) were used as the starting materials. In typical experiment, 0.98 gram of (NaOH, 98%) was dissolved in 24.56 ml distilled water to get 1.0 M. The resulting solution was heated under constant stirring at 70 ^oC. After obtaining the desired temperature, a solution of (Zn $(NO_3)_2.6H_2O$, 98%) (0.5 M in 24.56 ml water, 3.65g) was slowly added (dripping for 30 min) into the reactor. The resulting solution was remained agitated for a

period of two hours, maintaining the desired temperature. The material formed in the reactor was centrifuged by 5000 rpm for 20min, washed 3 times with distilled water and dried in oven at a maximum temperature of 70°C for 6 hours.

3.1.2 Combustion method

Combustion is defined as rapid oxidation generating either light or heat, or both of them in the case of fast oxidation (Bangale et al., 2013). This method has been extensively used to produce industrially useful materials. It is known as a versatile, simple and fast process, which offers effective synthesis of a variety of nanomaterials. The most important features that make the combustion method useful to prepare ZnO are the formation and crystallization of as prepared ZnO without need of thermal treatment.

In the present work, Zinc nitrate tetrahydrate ($Zn(NO_3)_2.4H_2O$, 98.5%) and urea ($CO(NH_2)_2$, 99%), were used as starting materials. Stoichiometric composition of zinc nitrates and fuel (Urea) were calculated depends on the total oxidizing and reducing valences as reported by Ekambaram and Patil (Ekambaram et al., 1997). In typical experiment, Zinc nitrate tetra-hydrate and urea were dissolved in distilled water. A homogenous solution was obtained after stirred the mixture for 20 min. The resulting solution was transferred to the muffle furnace maintained at temperature of 500 ^oC. In few minutes all water was evaporated and foaming followed by decomposition, generating large amount of gases. These combustible gases ignite and burn with a flame, yielding a large amount of solid. The resulting ZnO was cooled down and ground to fine powder.

3.2 Characterization techniques

It important to note that, all the measurements were done at the University of the Free State, South Africa.

3.2.1 X-ray Diffraction (XRD)

The X-ray diffraction (XRD) is known as an efficient non-destructive analytical technique used in solid state chemistry and material science. This technique had been discovered by von Laue in 1912. At that time, XRD was used only to determine crystal structure of matter. Later on, XRD was developed and successfully applied to study physical, chemical and mechanical properties of materials. As the results, XRD become an important characterization tools to identify many parameters such as phase, preferential orientation, texture, crystallite size, micro-strain and residual stress (Chai et al., 2010). In addition, XRD also provided information on unit cell dimensions. Crystal phases, size, shape and translational symmetry of the unit cell can be determined using peak position. Crystallite size, microstrain and residual stress are determined by peak shapes and widths while the peak intensities give information about preferential orientation. Although, other beams (e.g., ions, electrons, neutrons, and protons) were used, no one can replace the X-ray due their simplicity and cost effectiveness.

A diffraction pattern is produced when a material is irradiated with a collimated beam with specific wavelength of x-rays. The theoretical interpretation of x-ray diffraction from materials was explained by Bragg as will be discussed in the following section.

3.2.1.1 Bragg's law

It is well known that the diffraction is occur only if the interplanar spacing (d) of the crystal is of the same order of that of the x-ray wavelength. When the previous condition is satisfied, intense peaks of reflected x-ray will be produced. W. L. Bragg explained this result by modeling the crystal as a set of discrete parallel planes separated by a constant parameter d as shown in figure 3.1a. When a constructive interference occurs, a diffracted beam of X-rays will leave the crystal at an angle equal to that of the incident beam (figure 3.1b). This condition can be expressed by Bragg's law (Myers et al., 2002)

$$n\lambda = 2dsin\theta \qquad (3.1)$$

Where n is diffraction series, θ is diffraction angle, λ is the wavelength of X-ray and d is interplanar distance.

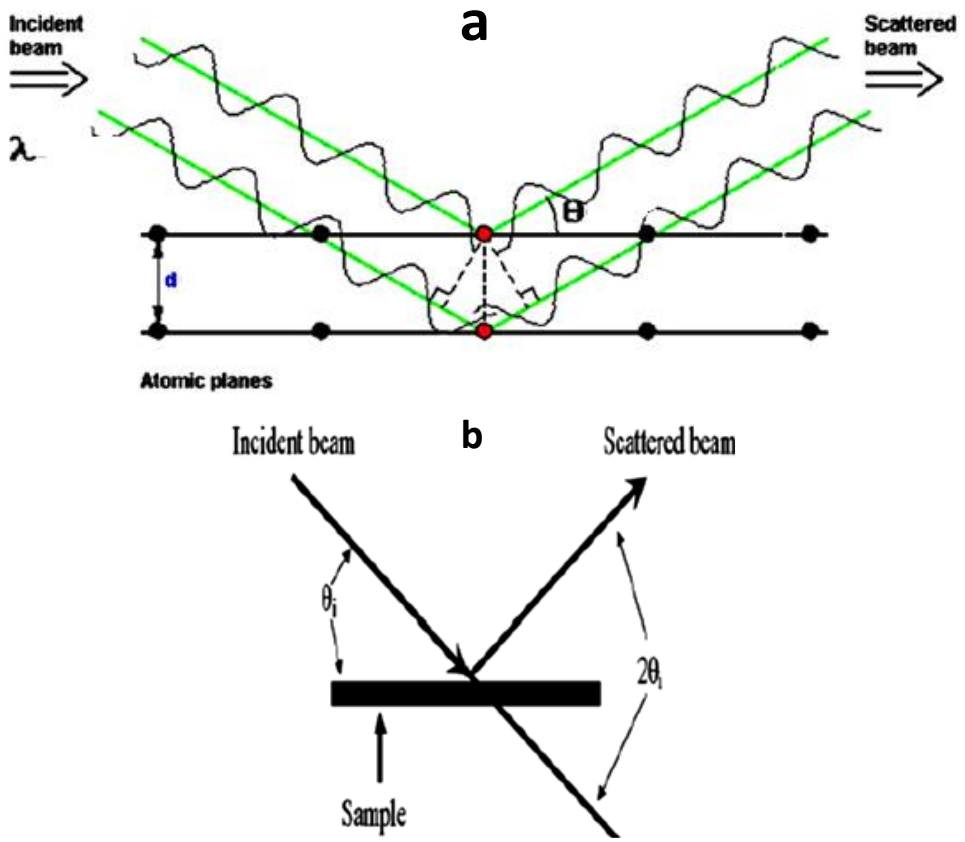

Fig. 3.1 (a) Schematic diagram of Bragg diffraction from a set of atoms (b) scattering of x-ray from sample (Kabongo et al., 2013).

The XRD data of this work were collected by a Bruker D8 diffractometer using CuKα (λ=1.5405 Å) radiation in the 2θ scan range of 15-90o and the X-rays were generated by applying 40 kV voltage on Cu anode material at a current of 40 mA.

3.2.2 Transmission Electron Microscopy (TEM)

TEM is an imaging technique whereby a beam of electrons is transmitted through a specimen, and then an image is formed. The image is then magnified and directed to appear either on a fluorescent screen or layer of photographic film, or to be detected by a sensor such as a CCD camera.

TEM is normally used to give detail information of bulk and nanomaterials using either imaging or diffraction pattern modes. It can investigate the size, shape and arrangement of the particles which make up the specimen as well as their relationship to each other on the scale of atomic diameters.

Materials to be analyzed with this technique need to have thickness small enoug h for electrons beam to penetrate the specimen.

A crystalline material interacts with the electron beam mostly by diffraction rather than absorption. The intensity of the transmitted beam is affected by the volume and density of the material through which it passes. The intensity of the diffraction depends on the orientation of the planes of atoms in a crystal relative to the electron beam. At certain angles the electron beam is diffracted strongly from the axis of the incoming beam, while at other angles the beam is largely transmitted. The possibility for high magnifications has made the TEM a valuable tool in medical, biological and material sciences research. In all cases, the specimens must be very thin and able to withstand the high vacuum present inside the instrument. In this study the images were obtained using a Philips CM100 TEM.

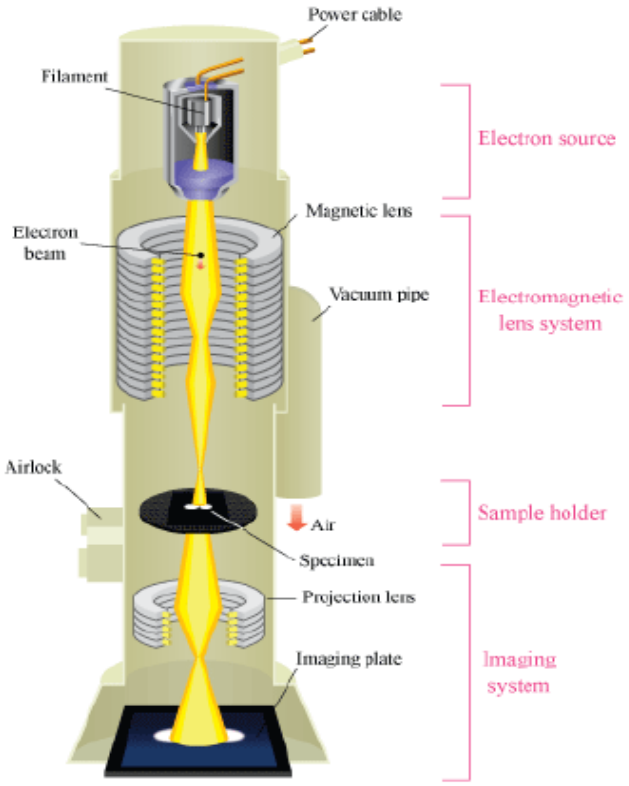

Fig.3.2 A schematic outline of a TEM (Damen et al., 1966).

3.2.3 Ultraviolet Visible Spectroscopy (UV-Vis)

The UV-Vis Spectrometer is one of most important technique in the modern day laboratories which is used to identify number of absorption species in sample. This instrument is commonly used to analyze compounds of organic, inorganic and biochemical in the ultraviolet and visible regions of electromagnetic spectrum. The UV-Vis spectrometers find a wide range of application in scientific research, industry, clinical laboratories and chemistry. The following diagram shows the main components of this instrument.

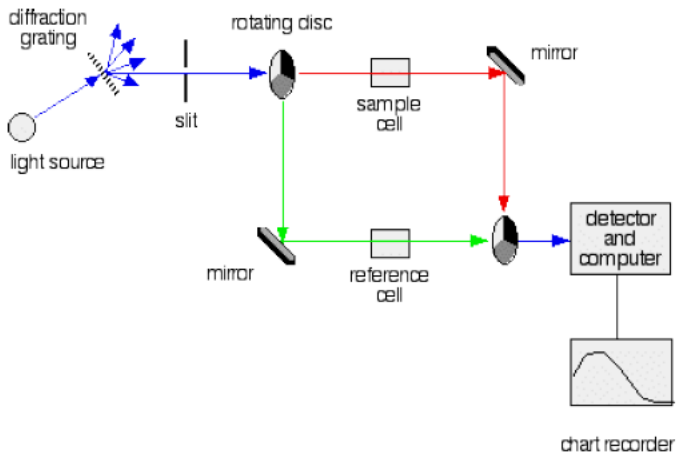

Fig.3.3 a dual-beam UV-Vis spectrophotometer (Morkoç et al., 2002).

The data produced by UV-Vis spectrometers can be obtained as either absorption or transmission spectrum. These two processes are based on the Lambert's Law which states that each layer of equal thickness of an absorbing medium absorbs an equal fraction of the radiant energy that traverses it. When light passes through a sample, the amount of light absorbed by the sample is the difference between the incident radiation (Marivone Gusatti and Humberto) and the transmitted radiation (I). The amount of light absorbed is expressed as either transmittance or absorbance. Transmittance is defined as (Lugo et al., 2010)

$$T = \frac{I}{I_o} \qquad (3.2)$$

While absorbance A is defined as

$$A = -logT \quad (3.3)$$

The main objective of this instrument in this work is to determine the energy band gap of ZnO.

3.2.4 Photoluminescence spectroscopy (PL)

Photoluminescence spectroscopy is a contactless, nondestructive method of probing the electronic structure of materials. Light is directed onto a sample, where it is absorbed and imparts excess energy into the material in a process called photo-excitation. One way this excess energy can be dissipated by the sample is through the emission of light, or luminescence. In the case of photo-excitation, this luminescence is called photoluminescence.

Photo-excitation causes electrons within a material to move into permissible excited states. When these electrons return to their equilibrium states, the excess energy is released and may include the emission of light (a radiative process) or may not (a nonradiactive process). The energy of the emitted light (photoluminescence) relates to the difference in energy levels between the two electron states involved in the transition between the excited state and the equilibrium state. The quantity of the emitted light is related to the relative contribution of the radiative process. In this study, the PL measurements were done using a 325 nm He-Cd laser as an excitation source and Horiba iHR320 mono-chromator attached with a PMT detector. Figure 3.4 shows a schematic diagram of a PL spectrophotometer with general basic equipment. In this instrument various sources may be used as an excitation source, namely lasers, photodiodes, and lamps. It is also provided with two mono-chromators to select both the excitation and emission.

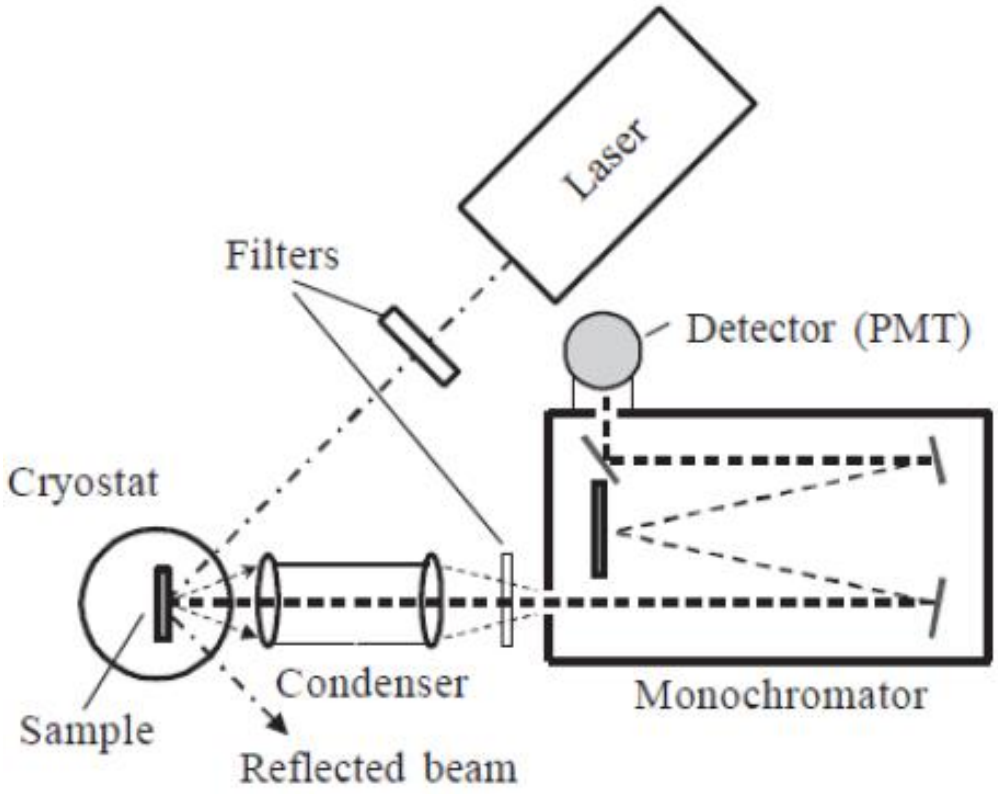

Fig. 3.4 Schematic diagram of a spectrofluorometer (Morkoç et al., 2008)

Chapter Four

Result and Discussion

4-1 Structure properties

4.1.1 X-rays diffraction studies

In this work, X-ray diffraction (XRD) technique was used to characterize the crystal structure, particle size, and lattice parameter for ZnO nanoparticles synthesized by two different methods namely combustion and sol-gel.

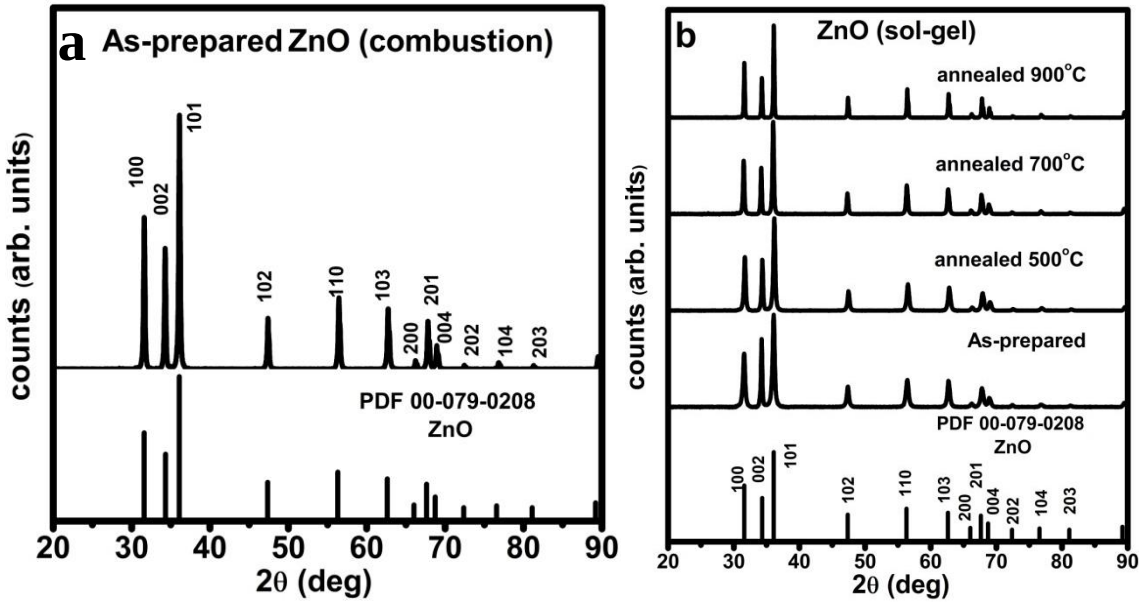

Fig.4.1 XRD pattern of ZnO nanoparticles synthesized by (a) combustion method (b) sol-gel method and annealed at different temperatures.

Figure 4.1a shows XRD diffraction pattern for as-prepared ZnO synthesized by combustion method. For comparison, The XRD pattern

obtained from as-prepared ZnO and ZnO annealed at different temperatures synthesized by sol-gel method is also presented in figure 4.1b. As can be seen from figure 4.1 (a & b) that all diffraction peaks assigned to crystalline of hexagonal ZnO with the wurtzite structure as compared with powder diffraction file (PDF 00-079-0208). Of interest is that there is no additional peaks of any other phase of ZnO or of any impurities are presented in all samples, indicating that both combustion and sol-gel methods are applicable to prepare ZnO with high crystallinity. For more structure details, the crystallite size and lattice parameter for all ZnO samples presented in figure 4.1 were calculated using Scherer's formula (see chapter 2, equation 2.1) and Bragg's formula (see chapter 2, equation 2.3), respectively. Table 4.1 showed the average crystallite size and the lattice parameter obtained from XRD spectra of ZnO synthesized by combustion and sol-gel method using the most intense peaks.

Table 4.1 average crystallite size and lattice parameter for ZnO synthesized by combustion and sol-gel method.

Material	Method	Annealing temperature (^{o}C)	Lattice parameter c/a (nm)	Crystallite size (nm)	Standard (ICSD, PDF 079-0208) c/a(nm)
ZnO	Combustion	As-prepared	1.586	33	1.598
ZnO	Sol-gel	As-prepared	1.588	22	
	Sol-gel	500 ^{o}C	1.588	24	
	Sol-gel	700 ^{o}C	1.586	32	
	Sol-gel	900 ^{o}C	1.584	45	

***Source: (analysis data, prepared by the researcher, 2018)**

As can be clearly seen from table 4.1 that the crystallite size of all ZnO samples are in nano-scale, indicating that both sol-gel and combustion

method can produce ZnO nanoparticles. In addition, the crystallite size of the ZnO synthesized by the sol- gel method increases by increasing the annealing temperature. It is also observed that there was little change in the lattice parameter when the annealing temperature was increased. This change in lattice parameters may be attributed to the change of particle size and quantum size effects. Of interest is that the crystallite size and lattice parameters for the ZnO synthesized with the combustion method are coincide with that of ZnO prepared with the sol-gel method and annealed at 700^{o}C, indicating that similar structure of ZnO can be obtained from both methods at particular conditions.

4.1.2 TEM studies

Although the Scherrer's equation has been applied extensively to calculate particle sizes from XRD spectra, it must still be considered as an approximate method due to other effects that comes from other parameters such as particle shape, particle size distribution and the strain. Therefore, calculation of the particle size from TEM images is preferable. Figure 4.2 is an image of the as-prepared ZnO synthesized by combustion method. It can be seen that the ZnO nanocrystals are irregularly spherical with average diameter of 32 nm (see the inset of figure 4.2), which is similar to the calculated crystallite size from the XRD data (see table 4.1). This may confirm that the value of particle sizes estimated by Scherrer's formula for all other ZnO samples are relatively precise.

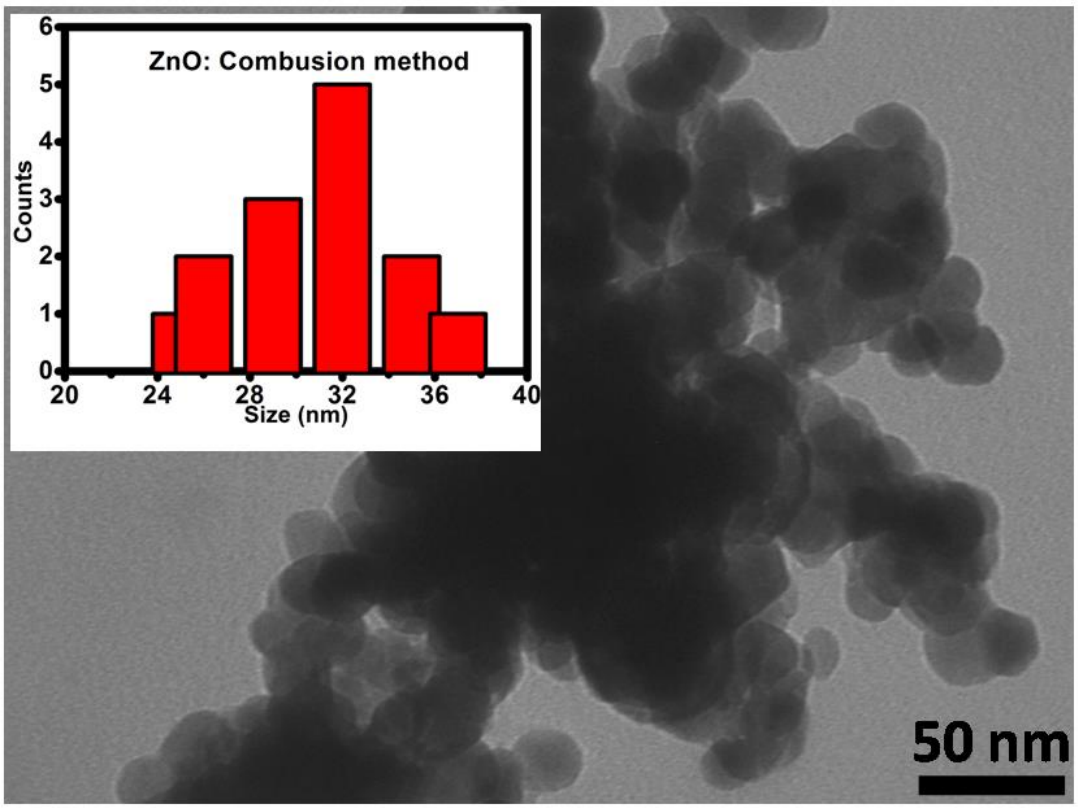

Fig. 4.2 TEM images of as-prepared ZnO nanoparticles synthesized by combustion method.

4.2 Optical studies

4.2.1 UV-Vis studies

The optical study of as-prepared ZnO synthesized by combustion method and ZnO prepared by sol-gel and annealed at different temperature has been completed with the UV visible spectroscopy. Figure 4.3 shows the UV–Vis reflectance spectra of the ZnO nanoparticles prepared (a) by combustion method (b) by sol-gel method and annealed at different

temperatures. As can be seen, the relevant decrease in the reflectance at wavelengths less than 400 nm can be attributed to the intrinsic band-gap absorption of ZnO due to the electron transitions from the valence band to the conduction band.

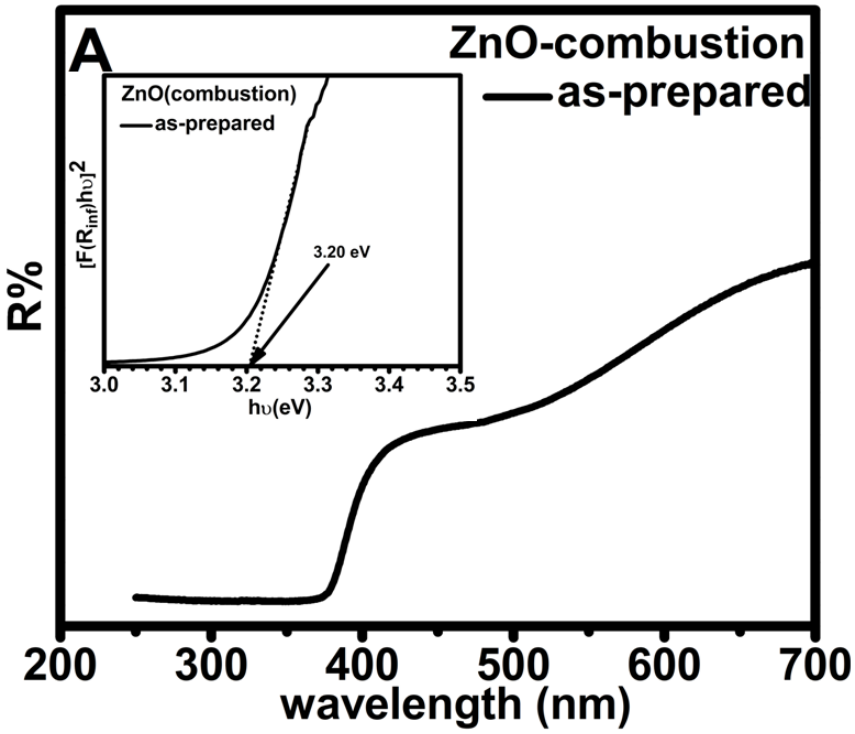

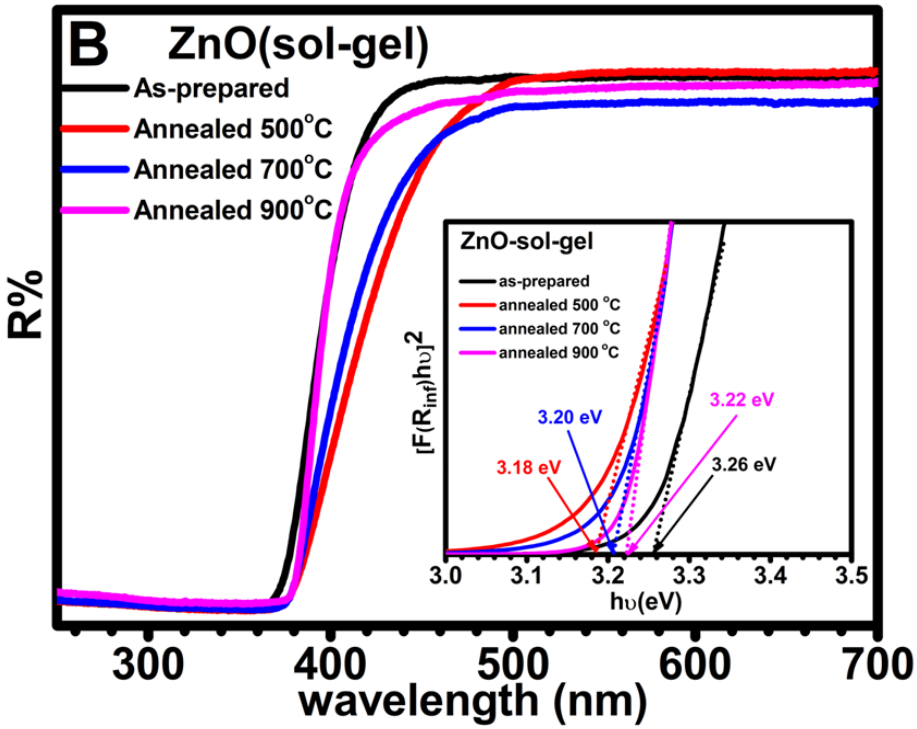

Fig.4.3 the UV–Vis reflectance spectra of the ZnO nanoparticles prepared (A) by combustion method (B) by sol-gel method and annealed at different temperatures.

To calculate the optical band gab of ZnO prepared by both methods, Kubelka-Munk equation (see chapter 2, equation 2.3) was applied. The energy bang gab of ZnO prepared by combustion method is found to be 3.2 eV (see the inset of Fig.4.3A). This is smaller than the energy band gap 3.37 eV of bulk ZnO. The blue shift in the band gab has been reported to be due to quantum confinement effect or the annealing temperature effect (Bodke M. R., 2014), while the red shift is assigned to changes in the morphologies, particle size, and surface microstructures (A. N. Mallika, 2015). For ZnO synthesized by sol-gel method, the calculated band gab was found to be increased by increasing annealing temperature from 500^{o}C to 900^{o}C (see the inset of Fig.4.3A). To understand the changes in the band gab as the function

of annealing temperature, the band gab values and particles sizes estimated from XRD are plotted against annealing temperature as shown in figure 4.4.

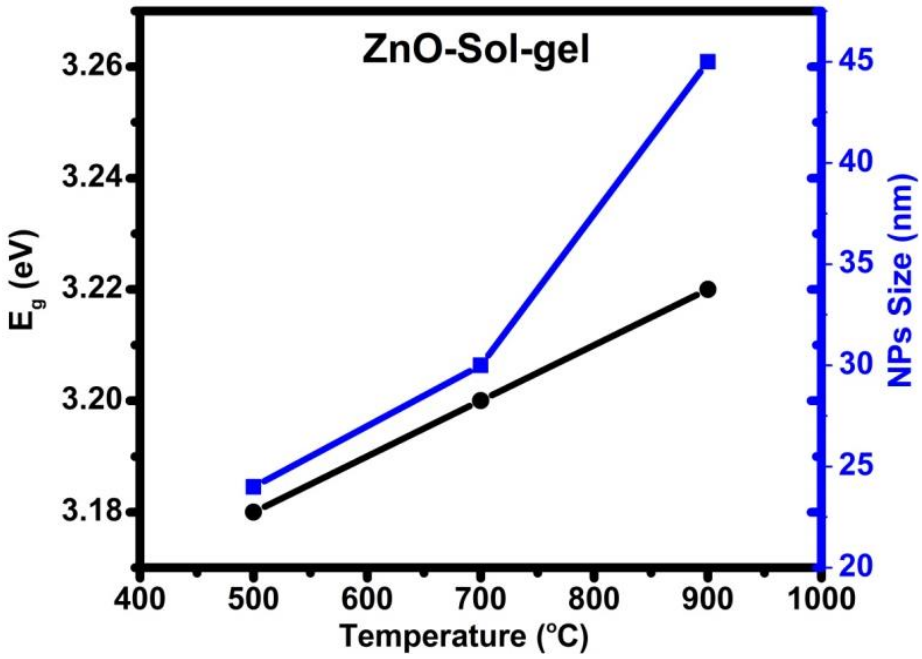

Fig. 4.4 Energy band gabs and particle sizes versus annealing temperatures

It can be seen that both the particle size and the band gab are increased by increasing annealing temperature. It is well known that in quantum size regime the band gab is increases by decreasing the particle size which is against the results observed in this work (see Figure 4.4). Therefore, the blue shift observed here may be due to reducing of ZnO defects as annealing temperature increased.

4.2.2 Photoluminescence Studies

The Photoluminescence spectroscopy is known as an effective method to investigate the presence of defects in semiconductor materials. Therefore, for comparison, two as-prepared ZnO samples synthesized by two different

methods were chosen to characterize by PL system using He-Cd laser as excited source as shown in figure 4.5.

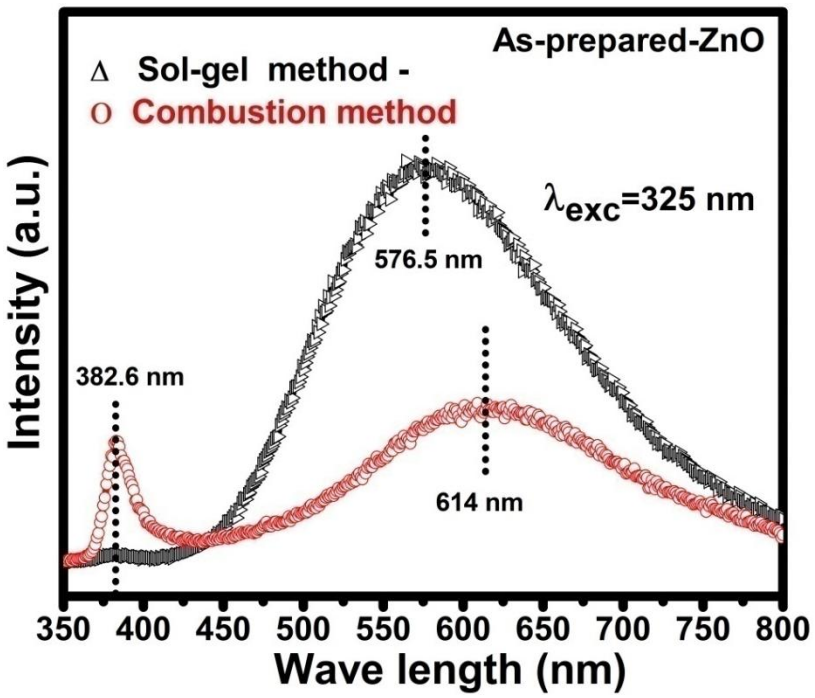

Fig. 4.5 PL spectra of as-prepared ZnO synthesized by sol-gel and combustion methods.

Figure 4.5 shows the room temperature PL spectra of as-prepared ZnO samples synthesized by two different methods. One of these samples was synthesized by sol-gel method while the other was prepared by combustion method. The spectra obtained from both samples showed sharp peak in UV region around 382.6 nm and abroad visible emission band located at 576.5 nm and 614 nm for the ZnO synthesized by sol-gel and combustion method, respectively. The peak located in the UV region is the so called near-band-edge emission which originates from free exciton emission while the broad

band emission is attributed to complicated defect related emissions [Ref]. It is also observed that the UV peak for the ZnO synthesized by combustion method is more pronounced than that of ZnO prepared by sol-gel, indicating the crystalline quality of the sample synthesized by combustion method. It is also seen that the broad band emission from ZnO prepared by sol-gel showed high intensity and different peak position compared with the peak observed from ZnO synthesized by combustion method. This indicates that the concentration and the type of defects in these two samples are mainly different. For more details about the defects in these two samples, the broad emission spectra of Fig. 4.5 were deconvoluted into two separate Gaussian peaks considering the position of main defects associated with ZnO reported in literature (Zakirov, 2017). Figure 4.6 shows PL spectra and deconvoluted bands for ZnO prepared by sol-gel and combustion method. For the sample prepared by combustion method there are two peaks located at 690 nm and 694 nm attributed to the transition of electron from Zn interstitial (Zn_i) to oxygen interstitial (O_i) and from oxygen vacancies (O_o) to valance band, respectively (Zakirov, 2017). Deconvolution of the PL spectrum obtained from ZnO synthesized by sol-gel method resulted into two peaks located at 567nm and 647 nm. The peak located at 567 nm is assigned to transition of electron from Zn interstitial to oxygen vacancies while the peak located at 647 is attributed to the transition of electron from conduction band to oxygen interstitial (M.I. Zakirov, 2017).

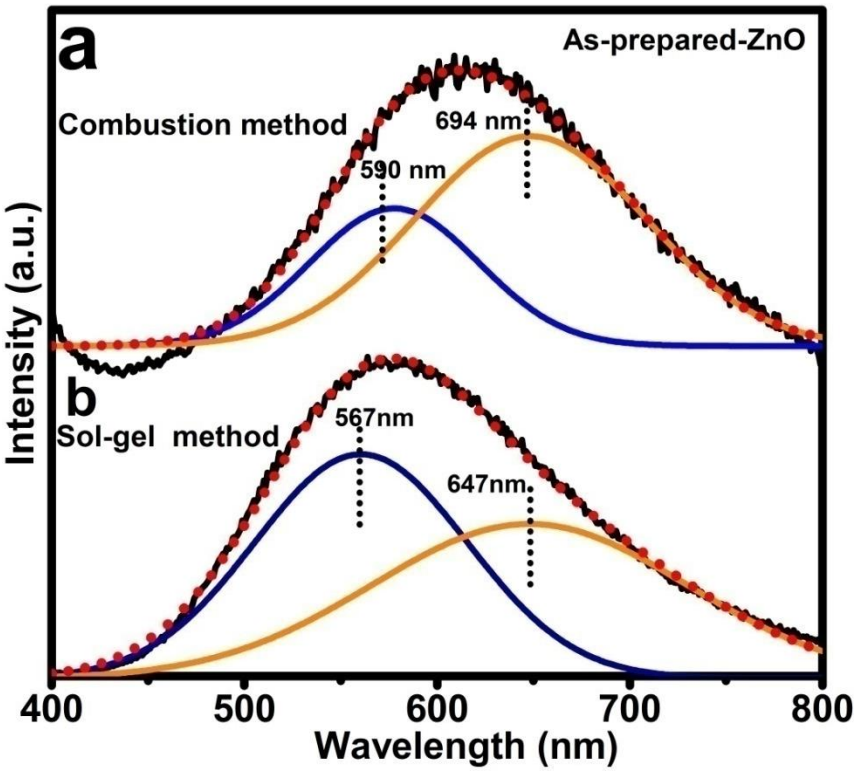

Fig. 4.6 PL spectra and deconvoluted bands for ZnO prepared by two different method

According to discussion above it is obvious that there is a clear difference between the two spectral obtained from ZnO synthesized by sol-gel and combustion method. This may be due to complicated defect chemistry relevant to the experimental process (the method used to prepare ZnO). Therefore, it can conclude that the concentration and the type of defect are basically associated with preparation method.

Chapter Five

Conclusion and future works

5.1 Conclusion

In this research, the structures and optical properties of un-doped Zinc oxide powders for both synthesized methods (combustion & sol-gel) were investigated. There is significant variation at properties was absorbed at comparative, and we conclude that:

- For structure properties the crystallite size of the ZnO synthesized by the sol- gel method increases by increasing the annealing temperature. There was little change in the lattice parameter when the annealing temperature was increased. The change in lattice parameters may be attributed to the change of particle size and quantum size effects.
- In addition the crystallite size and lattice parameters for the ZnO synthesized with the combustion method are coincide with that of ZnO prepared with the sol-gel method and annealed at 700^{o}C, indicating that similar structure of ZnO can be obtained from both methods at particular conditions.
- Moreover TEM studies show that the ZnO nanocrystals are irregularly spherical with average diameter of 32 nm, which is similar to the calculated crystallite size from the XRD data.
- For optical properties the energy bang gab of ZnO prepared by combustion method is found to be 3.2 eV, this is smaller than the

energy band gap 3.37 eV of bulk ZnO. For sol-gel method the particle size and the band gab are increased by increasing annealing temperature, this increasing due to the blue shift observed and it's may be due to reducing of ZnO defects as annealing temperature increased.

- We also conclude that there is a clear difference between the two spectral obtained from ZnO synthesized by sol-gel and combustion method, may be due to complicated defect chemistry relevant to the experimental process.
- The concentration and the type of defect are basically associated with preparation method.

5.2 Future works

As one of the most important applied compounds, there are many future works that related to zinc oxide such as:

- In this dissertation, the study was focus on the main defects of zinc oxide. As a future study, deeply study for all types of defects in zinc oxide.
- ZnO has a lot of physical and chemical properties as mentioned in chapter two, the studies of these properties will be done of the future works**.**
- Other techniques will be used to gather more information about the structural and optical properties of ZnO (I, e., SEM, HRTEM, XPS).

References

Aggelopoulos, C. A., Dimitropoulos, M., Govatsi, A., Sygellou, L., Tsakiroglou, C. D., & Yannopoulos, S. N. (2017). Influence of the surface-to-bulk defects ratio of ZnO and TiO2 on their UV-mediated photocatalytic activity. Applied Catalysis B: Environmental, 205, 292-301.

Alvi, N. H., Ul Hasan, K., Nur, O., & Willander, M. (2011). The origin of the red emission in n-ZnO nanotubes/p-GaN white light emitting diodes. Nanoscale research letters, 6(1), 130.

Anh, T. K., Loc, D. X., Tu, N., Huy, P. T., Tu, A., Minh, L., & Minh, L. Q. (2014). Wet Chemical Preparation of Nanoparticles ZnO: Eu3. Journal of Photonics, 2014.

Bangale, S. V., & Bamane, S. R. (2013). Preparation and electrical properties of nanostructured spinel ZnCr 2 O 4 by combustion route. Journal of Materials Science: Materials in Electronics, 24(1), 277-281.

Chu, S. Y., Yan, T. M., & Chen, S. L. (2000). Characteristics of sol-gel synthesis of ZnO-based powders. Journal of materials science letters, 19(4), 349-352.

Chai, J. H. J. (2010). Combining Zinc Oxide and Silver for Potential Optoelectronic Applications.

Chai, J. H. J. (2010). Combining Zinc Oxide and Silver for Potential Optoelectronic Applications.

Damen TC, Porto SPS and Tell B, Phys Rev 142 (1966) 570.

Dana, James Dwight; Hurlbut, Cornelius Searle (1959). Dana's Manual of Mineralogy (17th ed.). New York: Chapman Hall. pp. 78–89.

Gusatti, M., Rosário, J. A., Barroso, G. S., Campos, C. E., Riella, H. G., & Kunhen, N. C. (2009). Synthesis of ZnO nanostructures in low reaction temperature. CHEMICAL ENGINEERING, 17, 1017.

Hernandezbattez, A; Gonzalez, R.; Viesca, J.; Fernandez, J.; Diazfernandez, J.; MacHado, A.; Chou, R.; Riba, J. (2008). "CuO, ZrO2 and ZnO nanoparticles as antiwear additive in oil lubricants". Wear. 265 (3–4): 422–428.

Kabongo, G. L. (2013). Luminescence investigation of zinc oxide nanoparticles doped with rare earth ions (Doctoral dissertation).

Krongarrom, P., Rattanachan, S. T., & Fangsuwannarak, T. (2012). ZnO doped with Bismuth in case of in-phase behavior for solar cell application. Engineering Journal (Eng. J.), 16(3), 59-70.

Kumar, V., Prakash, J., Singh, J. P., Chae, K. H., Swart, C., Ntwaeaborwa, O. M., ... & Dutta, V. (2017). Role of silver doping on the defects related photoluminescence and antibacterial behaviour of zinc oxide nanoparticles. Colloids and Surfaces B: Biointerfaces, 159, 191-199).

Lugo, F. (2010). Synthesis and characterization of silver doped zinc oxide thin films for optoelectronic devices (Vol. 71, No. 08).

Mallika, A. N., Reddy, A. R., & Reddy, K. V. (2015). Annealing effects on the structural and optical properties of ZnO nanoparticles with PVA and CA as chelating agents. Journal of Advanced Ceramics, 4(2), 123-129.

McNeil, S. E. (2005). Nanotechnology for the biologist. Journal of leukocyte biology, 78(3), 585-594.

Myers. H. P. (2002). Introductory Solid State Physics. Taylor & Francis. ISBN 0-7484-0660-3.

Rodnyi, P. A., & Khodyuk, I. V. (2011). Optical and luminescence properties of zinc oxide. Optics and Spectroscopy, 111(5), 776-785.

Prabhu, Y. T., Rao, K. V., Kumar, V. S. S., & Kumari, B. S. (2013). Synthesis of ZnO Nanoparticles by a novel surfactant assisted amine combustion method. Advances in Nanoparticles,2(01), 45.

Savi, B. M., Rodrigues, L., & Bernardin, A. M. (2012). Synthesis of ZnO nanoparticles by sol-gel processing. Qualicer, 12, 1-8.

Shah, A. H., Manikandan, E., Ahmed, M. B., & Ganesan, V. (2013). Enhanced bioactivity of Ag/ZnO nanorods-A comparative antibacterial study. J. Nanomed Nanotechol, 4(3), 2-6.

Singh, N. S., Singh, S. D., & Meetei, S. D. (2014). Structural and photoluminescence properties of terbium-doped zinc oxide nanoparticles. Chinese Physics B, 23(5), 058104.

Siva Vijayakumar, T., Karthikeyeni, S., Vasanth, S., Ganesh, A., Bupesh, G., Ramesh, R., ... & Subramanian, P. (2013). Synthesis of silver-doped zinc oxide nanocomposite by pulse mode ultrasonication and its characterization studies. Journal of Nanoscience, 2013.

Suwanboon, S. (2008). Structural and optical properties of nanocrystalline ZnO powder from sol-gel method. Science Asia,34(1), 31-34.

Teng, X. M., Fan, H. T., Pan, S. S., Ye, C., & Li, G. H. (2006). Influence of annealing on the structural and optical properties of ZnO: Tb thin films. Journal of applied physics, 100(5), 053507.

Van Nghia, N., Trung, T. N., Truong, N. N. K., & Thuy, D. M. (2012). Preparation and Characterization of Silver Doped ZnO Nanostructures. Open Journal of Synthesis Theory and Applications, 1(02), 18.

Vaseem, M., Umar, A., & Hahn, Y. B. (2010). ZnO nanoparticles: growth, properties, and applications. Metal oxide nanostructures and their applications, 5, 1-36.

Welderfael, T., Yadav, O. P., Taddesse, A. M., & Kaushal, J. (2013). Synthesis, characterization and photocatalytic activities of Ag-N-codoped ZnO nanoparticles for degradation of methyl red. Bulletin of the Chemical Society of Ethiopia, 27(2), 221-232.

Zakirov, M. I., & Korotchenkov, O. A. (2017). Carrier recombination in sonochemically synthesized ZnO powders.Materials Science-Poland, 35(1), 211-216.